*Proceedings of the*
*Annual Stability Conference*
*Structural Stability Research Council*
*Atlanta, Georgia, April 21-24, 2020*

# Stability of speedcore walls under fire loading: summary of numerical analyses

Ataollah Taghipour Anvari[1], Saahastaranshu R. Bhardwaj[2], Preshit Wazalwar[3], Amit H. Varma[4]

## Abstract

Concrete-Filled Composite Plate Shear Walls (C-PSW/CF), also known as SpeedCore, are being considered for commercial buildings due to the benefits of modularization and schedule contraction. For building design and applicability evaluation of these walls, the stability of C-PSWs/CF under fire loading needs to be evaluated. During a fire event, the steel plates will be directly exposed to fire. The high temperatures result in the degradation of material strength and stiffness which may lead to the collapse of walls under gravity loads. Thermal and structural finite element models were developed and benchmarked to the existing database of standard fire tests conducted on scaled C-PSWs. The authors conducted analytical parametric studies using the benchmarked finite element models. A unit-width column strip method of analysis for walls is introduced and evaluated. C-PSWs/CF with various wall slenderness (height-to-thickness) ratios and wall thicknesses were studied. The applied gas temperatures were based on ISO 834 standard time-temperature curves. The models underwent thermal expansion upon application of fire loading resulting in cracking of infill concrete. The degradation in material properties and cracking of concrete resulted in local buckling of the steel plates between the ties (or shear studs). Continued fire exposure led to significant degradation of material properties and failure of walls due to crushing or global instability. Wall slenderness and wall thickness have a significant effect on the fire resistance of C-PSWs/CF. An increase in the wall thickness results in a higher failure time for walls, while a higher wall slenderness ratio results in a lower failure time. The parametric study (and existing experimental) results are used to develop design recommendations and compression strength equations for C-PSWs/CF under fire loading. These recommendations will be beneficial to the industry for the fire evaluation and design of C-PSWs/CF.

## 1. Introduction

Concrete filled composite plate shear walls (C-PSWs/CF) are gaining popularity for commercial construction due to the advantages of modularity and schedule construction. The C-PSWs/CF include plain concrete (concrete infill) sandwiched by steel plates (faceplate). Steel plates are connected to each other through tie bars. The steel plates act as primary reinforcement. Tie bars ensure the structural integrity of the system (Seo et al. 2016) and serve as out-of-plane

[1] Graduate Research Assistant, Purdue University <ataghipo@purdue.edu>
[2] Assistant Professor, The University of Alabama <saahas.bhardwaj@ua.edu>
[3] Graduate Research Assistant, Purdue University <pwazalwa@purdue.edu>
[4] Karl H. Kettelhut Professor and Director of Bowen Laboratory, Purdue University <ahvarma@purdue.edu>

reinforcement (Bhardwaj and Varma 2017a). The composite action between steel plates and concrete infill can be provided by ties (and shear studs) welded on the inside surface of the steel plates. Significant research has been done in the recent past to study the behavior and design of C-PSWs/CF (known as SC walls). The research and design provisions have been discussed in detail by Bhardwaj and Varma (2017b).

The fundamental behavior for commercial building application of C-PSWs/CF was studied by Selvarajah (2013), Bruneau et al. (2013), Ji et al. (2017), and Varma et al. (2017). The current building codes, i.e. ASCE 7 (2016) and AISC 341 (AISC 2016) permit the use of C-PSW/CF in seismic regions (Bruneau et al. 2013, Alzeni and Bruneau 2014, Epackachi et al. 2015, Kurt et al. 2016, Bhardwaj et al. 2018a). Varma et al. (2019) evaluated the stability of empty steel C-PSWs/CF modules. Wang et al. (2018) investigated the lateral capacity of C-PSWs/CF for wind and seismic loads. Bhardwaj and Varma (2016, 2017) have developed a procedure to quantify the effects of initial imperfections and concrete casting pressure on the compression behavior of C-PSWs/CF. Bhardwaj et al. (2018b) also recommended a steel plate (web plates and flange plate) slenderness criteria for C-PSWs/CF.

A significant step towards formalizing the use of C-PSWs/CF in commercial construction requires an understanding of the stability of C-PSWs/CF at elevated temperatures, and development of fire resistance ratings and strength equations at elevated temperatures. The elevated temperatures due to fire will result in degradation of the mechanical properties of steel and concrete. Degraded material properties may cause local or global instability or global crushing failure at load levels lower than the design loading. Hence, experimental and numerical studies are needed to evaluate the stability of C-PSWs/CF under fire loading.

There are some recent studies investigating the behavior of C-PSWs/CF at elevated temperatures. Wei et al. (2017) experimentally tested concrete-filled steel plate composite walls (CFSPC) under fire loading. These studies have been utilized for the development of benchmarked models used for the parametric studies presented in this paper. Wei et al. (2017) investigated the fire resistance of 12 concrete-filled steel plate composite (CFSPC) wall specimens. The specimens tested had a range of values for parameters such as steel plate thickness, wall height, wall thickness, the spacing of shear studs, fire scenario, and load ratio. The gas temperature was controlled to follow the ISO 834 (ISO 1975) standard time-temperature curve. Uniform and single-sided fire tests were performed. The specimen height varied from 850 to1850 mm. The width of the specimens was maintained at 1000 mm. Specimens had different shear stud/tie bar spacing (40, 60 and 80 mm). Stud and tie bar diameters were 2 and 10 mm, respectively. The specimens were embedded in the loading beam and the base beam at the top and bottom, respectively. Specimens were connected to the strong floor through the base beam. A constant axial load was applied to the top walls during the tests. Eight specimens were exposed to fire at all the four sides of the specimens. The remaining four specimens were tested for single-sided fire scenarios. Local buckling, weld cracking, and global instability were the limit states observed in the specimens before failure. The results indicated that the specimen slenderness ratio (wall height-to-thickness ratio) has a significant effect on the behavior of CFSPC walls. Specifically, as the slenderness ratio of specimens increases, the fire resistance of specimens decreases. An increase in the wall height also changes the failure mode from crushing failure to global instability failure. The thicker specimens had a higher fire resistance.

Moon et al. (2009) have tested stiffened steel plate concrete walls at elevated temperatures. Ribs were used on steel plates to improve the stability of steel plates. The wall specimens were exposed to fire on one face only (single-sided fire) for different axial load values. The fire temperatures were applied according to ISO 834 standard fire-temperature curve. The effect of applied axial load ratios was studied. The specimens subjected to higher load ratios failed sooner. The specimens initially experienced a lateral displacement towards the exposed surface but started buckling in the other direction (towards the unexposed face) at later stages. Local bulging of surface steel plates, spalling of concrete, and stud/tie weld rupture were observed at the failure of the specimens.

Varma et al. (2013) investigated the local buckling behavior of SC Composite walls. The walls were analyzed at both ambient and elevated temperatures. Benchmarked FE models were used to assess the performance of the walls subjected to a combination of thermal and gravitational loads. Parametric studies were also conducted to analyze the response of the wall specimens by varying the steel plate slenderness (stud spacing-to- steel plate thickness ratio) and the applied temperature (up to 350$^{o}$C). The researchers observed that the existing design provisions for compression strength of SC walls were marginally unconservative for temperatures above 250 $^{o}$C.

## 2. Benchmarked Finite Element Models

Finite Element (FE) analysis was utilized to study the stability of C-PSWs/CF under fire loading. Three-dimensional transient thermal and structural finite element models were developed using ABAQUS (Simulia, 2016). Sequentially coupled thermal-stress analysis was used. Temperature-dependent thermal and structural material properties were used for the models per Eurocode 4 (2005). The FE models were benchmarked to the experimental tests conducted by Wei et al. (2017). The development and benchmarking of the models have been previously discussed by the authors (Bhardwaj et al. 2019). In the current study, the benchmarked modes have been used to perform a parametric study for C-PSWs/CF under fire loading.

*Thermal finite element models*

The thermal heat transfer analysis comprised the steel plates and concrete infill. The concrete infill was modeled using DC3D8 element, which is an 8-node linear heat transfer brick element, and the steel plates are modeled using DS4 element. Based on calibration studies for heat transfer results, moisture content of 3% was selected and the specific heat was chosen accordingly. The average of upper and lower limit values of thermal conductivity specified by the Eurocode was used for concrete. The thermal expansion values of siliceous aggregate concrete were used. The faceplate was conservatively tied to the exterior surface of concrete-infill and the energy loss at the steel-concrete interface was not considered. This approach is conservative as it may result in slightly higher temperatures through the thickness of specimens than the experimentally measured temperatures. The specimens were subjected to ISO-834 standard fire curve (ISO, 1975). The steel surface temperatures were defined using the 'FILM' subroutine in ABAQUS. The subroutine accounts for heat transfer through radiation and convection. The details of the subroutine are reported by Cedeno et al. (2009).

For specimens tested by Wei et al. (2017), the measured surface and the mid-thickness temperatures of the concrete infill were compared with those obtained from FE analysis (Fig. 1). The comparison of results for only two walls (SCW4 and SCW7) is shown for brevity. For SCW4, the surface temperature at 2.5 hours of heating was 971°C. The temperature at the center of the

wall at this time was 610°C. For SCW7, the corresponding temperatures were 1010°C and 745°C respectively. The mid-thickness temperatures obtained numerically compare well with the measured temperatures for both specimens. The measured surface temperatures indicate a plateau at the beginning of the fire test. The plateau may be due to heat expended in vapor formation or inconsistencies in the measurements. Also, the surface temperature is reported at 2 mm from the concrete surface and the steel surface temperatures are not reported.

The numerically obtained surface temperature distribution was marginally higher than the measured temperature profiles. This may be due to the air gap between the faceplate and concrete surface upon initiation of the local buckling of the faceplate. FE models do not account for any heat loss at the steel-concrete interface. The higher surface temperature in FE analysis can decrease the failure time of the specimens. However, considering potential variability in experimental observations, using the ISO 834 fire curve is a more reliable and conservative approach to determine the failure time and surface temperature for C-PSWs/CF.

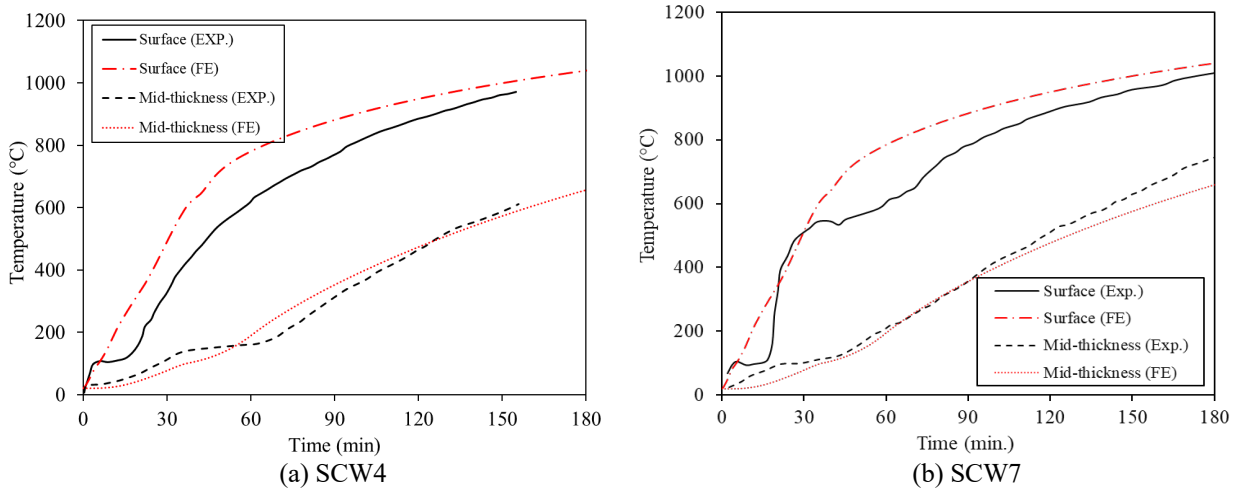


(a) SCW4 (b) SCW7

Figure 1: Comparison of predicted temperatures from the FE analysis with the experimental (Exp.) data

*Stress finite element analysis*

The stress models were developed to be consistent with the thermal model (e.g., the same mesh sizes were used for both models). The concrete infill, faceplates, shear studs and tie bars were explicitly modeled. The concrete infill was modeled using C3D8R solid element, an 8-node linear brick element with reduced integration. Concrete damaged plasticity model was used to simulate the behavior of concrete at elevated temperatures. The steel plates (faceplate) were modeled using S4R shell element, a 4-node general-purpose linear shell element. Since the faceplate had a very small thickness compared to the concrete infill's thickness, using shell elements was appropriate to capture any buckling in the faceplate. Also, using shell elements makes sequentially coupled thermal-stress analysis computationally efficient. The elastic-plastic stress-strain model was utilized for steel material. Hard contact and tangential behavior with a friction coefficient of 0.55 was used to define the contact properties between the faceplate and concrete-infill of the models.

The tie bars and shear studs (connectors) were modeled using B31 elements. B31 element is a 2-node linear beam element. The force-slip relationship for connectors was calculated based on the proposed relation by Ollgaard et al. (1971). Cartesian type connector elements were employed to

simulate the temperature-dependent force-slip behavior of studs and ties. The force-slip relationship for connectors was modified to consider temperature-dependent properties as discussed by Selden (2014). Connectors were embedded in the concrete infill. A rigid body constraint was applied to the top surface of the models. The bottom surface was restrained for all degrees of freedom. Pinned boundary condition was applied to the reference node assigned to the model's top surface rigid body. The stress analysis comprised of two steps. In the first step, the axial load's magnitude was increased from zero to the maximum value in an hour. In the second step, the nodal temperatures (based on heat transfer analysis) were applied until failure while the axial load magnitude was maintained constant.

The measured axial displacements were compared with numerically obtained axial displacements. Fig. 5 shows the comparison of axial deformation for benchmarked FE models of SCW4 and SCW7 (walls). The specimens experienced thermal expansion at the beginning of the fire test, resulting in the cracking of concrete-infill. The mechanical properties of concrete and steel material degrade at elevated temperatures. The models then underwent axial compression and shortening leading to the failure of the specimens. The numerically obtained axial displacements are in good agreement with measured displacements and the failure of specimens was well predicted.

*FE models of a strip of C-PSWs/CF (columns)*

The experiments by Wei et al. (2017) considered all-sided fires. However, C-PSWs/CF for buildings will typically have widths significantly more than the thickness, and be subjected to two-sided (both webs) or one-sided (one web, where the wall may need to design as a fire barrier) fire. The variation of through-thickness temperatures along the width of the wall will be negligible (except corner regions for C-shaped walls). Therefore, the possibility of unit-width analyses of C-PSWs/CF for fire loading needs to be explored. The walls can then be analyzed as unit width column strips, and design strengths can be provided per unit width of the wall.

C-PSWs/CF may be designed with different configurations like planar walls or C-shaped walls. The interior region can be conservatively modeled as the unit width column representing the whole wall because the regions of the wall closer to boundary elements may have higher axial compression stiffness and strength than the interior regions. The schematic distribution of critical axial compression capacity of a C-shaped C-PSW/CF is shown in Fig. 2. This was verified by comparing the axial load distribution in different regions of the walls during the heating. A rigid constraint was applied to the top surface of walls in the FE models. The axial load was uniformly applied along the width of the walls. The cross-section of a simulated wall with boundary elements was divided into three regions along the width (middle and ends). The normalized axial reaction (at the base) of the concrete infill and faceplate in the middle and the end parts for SCW4 is compared in Fig. 3. The axial reactions were almost the same at ambient temperature for both regions. At the beginning of the analysis, the model undergoes thermal expansion leading to concrete cracking. Thus, the axial force in concrete infill dropped and the majority of the applied load was transferred to faceplate. However, after about 40 min due to the reduction of stiffness and local buckling of faceplate at elevated temperatures, the applied axial load gradually transferred to concrete infill. The summation of base reaction forces in the middle region was lower than at the ends throughout the fire loading. Thus, the column strip taken from the middle region of the wall can be used to conservatively estimate the strength of the wall at elevated temperatures.

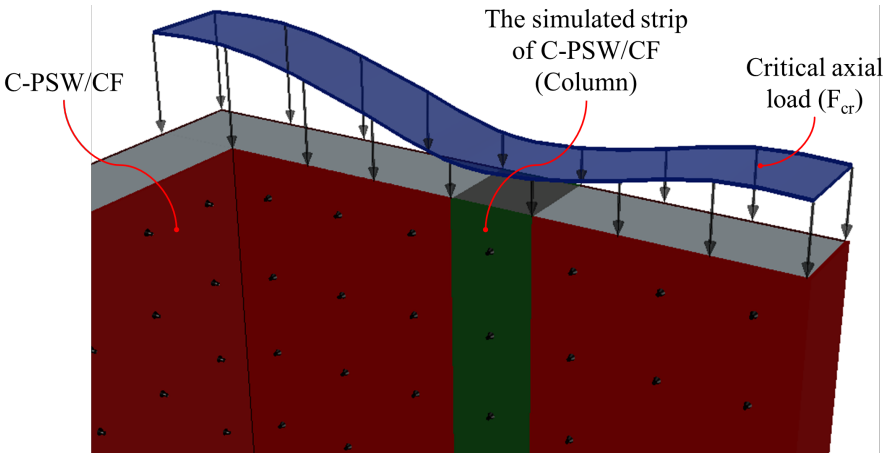


Figure 2: The variation of critical load of a for different parts of a C-PSW/CF along the wall length.

The FE models benchmarked to tests by Wei et al. (2017) were used to simulate a unit width strip of C-PSWs/CF (column) representing the middle region of the wall. The models included a row of tie bars and shear studs. The width of the models was equal to the tie bar spacing. The faceplate was modeled on two sides of the wall. The elevated temperatures were applied to two sides (faceplates) assuming the heat flow is perpendicular to the width of the wall. Symmetric boundary conditions were applied to the edges of the faceplate. The transitional degree of freedom along the wall width was not restrained to allow the column to expand along its width at elevated temperatures. A 3-D view of the developed FE model is shown in Fig. 4.

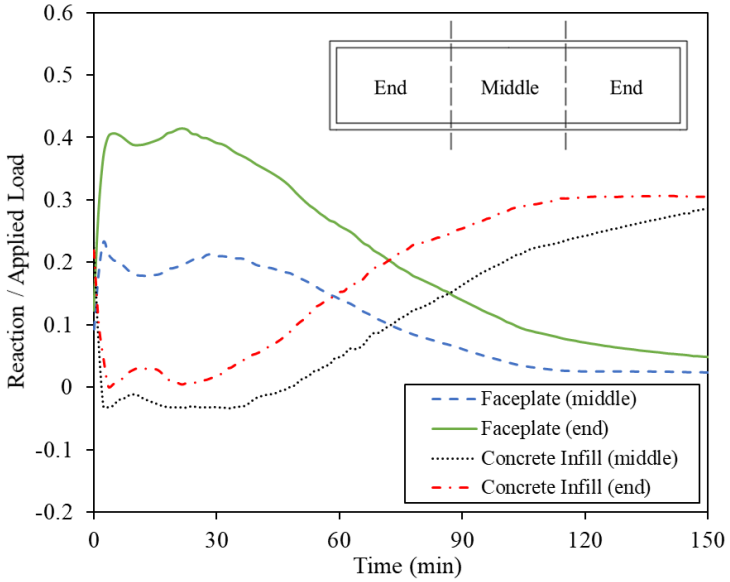


Figure 3: Distribution of axial load between the middle and end regions in SCW4

The axial displacement of the column strip models is compared with the modeled walls and experimental data in Fig. 5. A comparison of the failure times of the benchmarked models is presented in Table 1. The columns strip models gave comparable results to the wall models and the experimental results. The failure times for the column strip models are lower than those for the experiments and wall strip models. The failure time of SCW4 (wall) was 155 min which was

reduced to 139 mins for the column strip model. The simulated columns have lower axial capacity as was discussed earlier. However, the general behavior is in good agreement with the experimental behavior. The column strip method can be used to conservatively analyze and design C-PSWs/CF with varied configurations and dimensions.

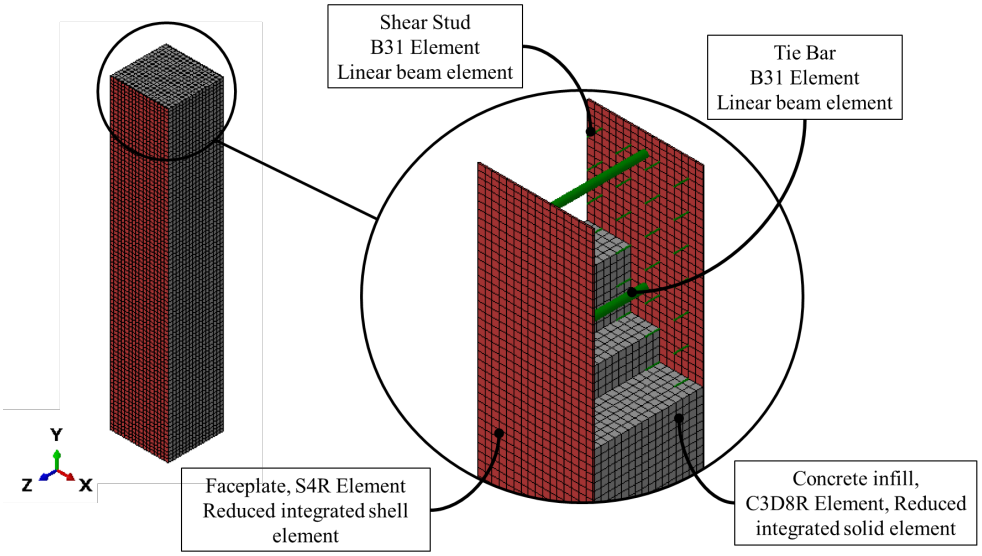


Figure 4: The developed three-dimensional model of a strip of C-PSW/CF (column)

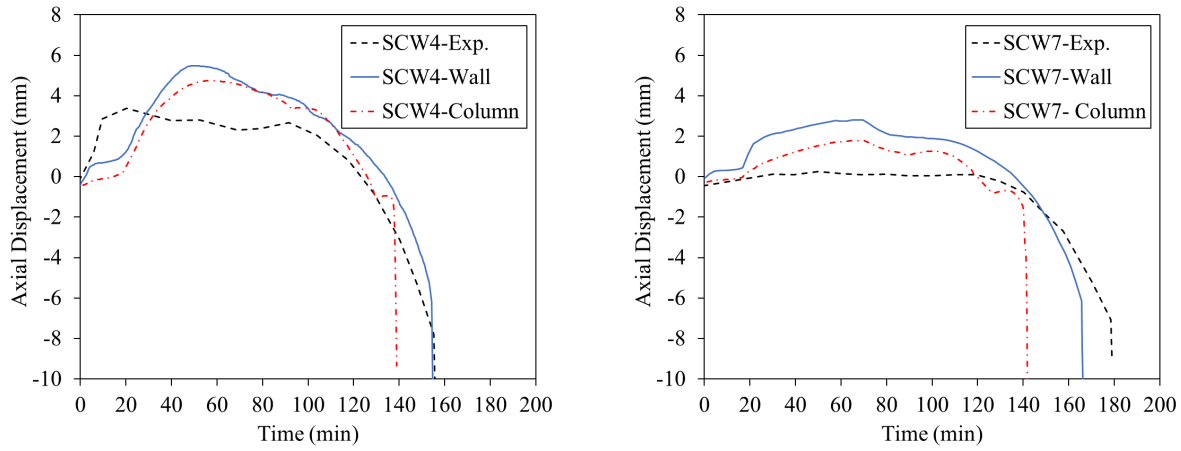


(a) (b)

Figure 5: Comparison of numerically obtained axial displacements with experimental data

Table 1: Summary of finite element and experimental results (specimens tested by Wei et al. 2017)

| Specimens | $H$ (mm) | $T$ (mm) | $t_p$ (mm) | Shear stud | Tie bar | Load Ratio | Failure Time (min) | | |
|---|---|---|---|---|---|---|---|---|---|
| | | | | | | | Test | FE (Wall) | FE (Column) |
| SCW4 | 1350 | 150 | 3 | Φ2@40 | Φ10@160 | 0.34 | 156 | 155 | 139 |
| SCW7 | 850 | 150 | 2 | Φ2@40 | Φ10@160 | 0.40 | 178 | 166 | 142 |

All dimensions in mm, unless noted otherwise.

## 3. Analytical Study Matrix

Table. 2 presents the details of models considered in the parametric study. The table also summarizes the failure time and temperature for the models. The range of parameters considered for the study is based on current industry practice and literature recommendations (AISC 2016, Varma et al. 2014). The wall slenderness ratio (wall height-to-thickness ratio) and wall thickness are the parameters considered in this study. The wall slenderness and wall thickness considered ranged from 5-20 and 200-400 mm, respectively. The faceplate thickness ranged from 4 to 8 mm and was changed to maintain a constant steel plate reinforcement ratio (4%) in all cases. Tie bars with a diameter of 7 mm to 20 mm were modeled at a distance equal to half of the wall thickness (*T/2*). The tie bar's diameter was selected to provide a shear reinforcement ratio of 0.35 for all walls. The steel plate slenderness was limited to 28.9 ($1.2\sqrt{E/F_y}$). The applied axial load was equal to 20% compressive axial capacity of concrete infill ($0.20A_g f'_c$). Pinned-pinned boundary condition was considered.

## 4. Parametric Study Results

The evolution of through-thickness temperature distribution for 200 and 300 mm thick walls is shown in Fig. 6. The non-linear temperature distribution is symmetric through the thickness. The mid-thickness temperature of the walls is dependent on the wall thickness. After 4-hour heating of the walls, the mid-thickness temperature of 200 and 300 mm thick walls are 548°C and 256°C, respectively. However, the surface temperatures of these walls are similar throughout the fire duration.

Table 2: Properties of models studied in the parametric study

| Nomenclature | $T$ *(mm)* | $H$ *(mm)* | $H/T$ | Load ($P_n/A_c f'_c$) | $t_p$ (*mm*) | $d_{tie}$ *(mm)* | $2t_p/T$ | $S_{tie}/T$ | Failure time (min) | Failure temperature (°C) |
|---|---|---|---|---|---|---|---|---|---|---|
| CW-200-05-20P | 200 | 1000 | 5.00 | 20% | 4 | 7 | 4.00% | 0.5 | 198 | 1105 |
| CW-200-10-20P | 200 | 2000 | 10.00 | 20% | 4 | 7 | 4.00% | 0.5 | 160 | 1068 |
| CW-200-15-20P | 200 | 3000 | 15.00 | 20% | 4 | 7 | 4.00% | 0.5 | 112 | 1004 |
| CW-200-20-20P | 200 | 4000 | 20.00 | 20% | 4 | 7 | 4.00% | 0.5 | 81 | 943 |
| CW-300-05-20P | 300 | 1500 | 5.00 | 20% | 6 | 10 | 4.00% | 0.5 | 353 | 1197 |
| CW-300-10-20P | 300 | 3000 | 10.00 | 20% | 6 | 10 | 4.00% | 0.5 | 250 | 1140 |
| CW-300-15-20P | 300 | 4500 | 15.00 | 20% | 6 | 10 | 4.00% | 0.5 | 140 | 1041 |
| CW-300-20-20P | 300 | 6000 | 20.00 | 20% | 6 | 10 | 4.00% | 0.5 | 122 | 1016 |
| CW-400-05-20P | 400 | 2000 | 5.00 | 20% | 8 | 14 | 4.00% | 0.5 | 584 | 1276 |
| CW-400-10-20P | 400 | 4000 | 10.00 | 20% | 8 | 14 | 4.00% | 0.5 | 446 | 1234 |
| CW-400-15-20P | 400 | 6000 | 15.00 | 20% | 8 | 14 | 4.00% | 0.5 | 209 | 1110 |
| CW-400-20-20P | 400 | 8000 | 20.00 | 20% | 8 | 14 | 4.00% | 0.5 | 171 | 1075 |

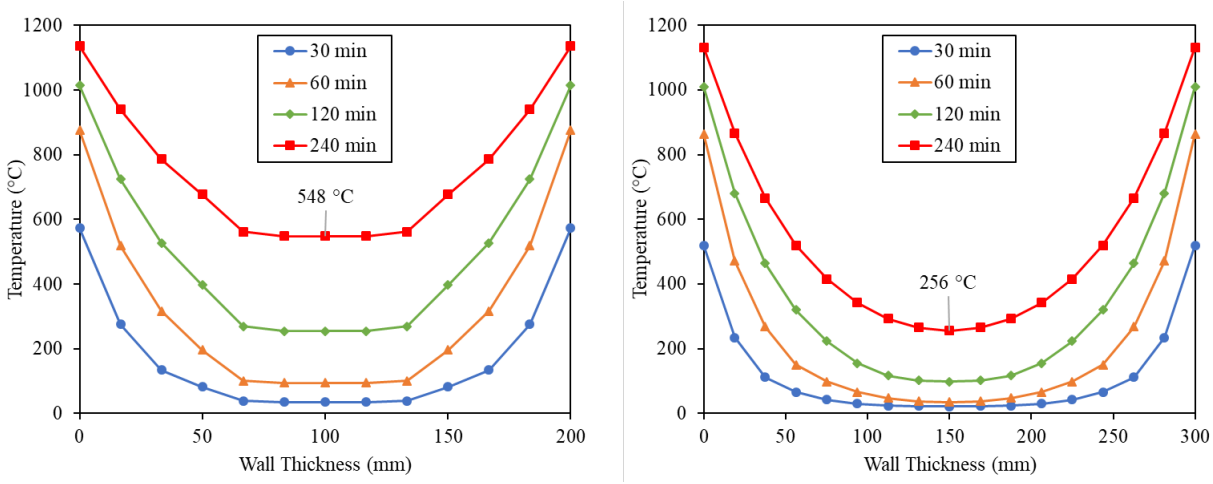


(a) CW-200 (b) CW-300

Figure 6: Comparison of the temperatures through the thickness of C-PSWs/CF at different time steps

The behavior of all the models under fire loading was similar. At early steps of fire exposure, walls experienced thermal expansion. The concrete infill cracked due to the expansion and the axial load was primarily resisted by steel plates. The extent of expansion depended on the height of the wall such that shorter walls expanded less than the taller walls (as seen in Fig.7). Elevated temperatures led to degradation of material properties resulting in local buckling of the faceplates. Upon buckling, the concrete started picking up compressive stress and the steel contribution reduced due to a significant reduction in material properties at elevated temperatures. With increasing duration of the fire, through-thickness temperatures increase (Fig.6), leading to degradation of material properties, increased rate of in axial shortening, and failure of the walls.

The axial displacement against time plots for the walls are presented in Fig.7(a). The results show that an increase in the wall slenderness ratio results in a lower failure time (CW-300-10-20P failed at 250 mins while CW-300-15-20P failed at about 140 mins). The failure was considered when the axial deformation exceeded *L/100* (mm), where *L* is the height of the wall (ISO 834, 1975). CW-300-10-20P failed due to the crushing of the cross-section, whereas CW-300-15-20P failed due to global instability. Fig.7(b) shows the axial displacement against surface temperature plots for the models. Models with a higher wall slenderness ratio failed at lower surface temperatures, however, the failure surface temperature was greater than 1000°C for all the walls.

The thickness of C-PSWs/CF had a major influence on the failure time of the walls. A comparison response of 200 mm and 300 mm thick walls (with same slenderness ratios) indicated that reducing the wall thickness led to lower failure times. Due to the low thermal conductivity of concrete, the middle of concrete in thicker walls (300 min) was cooler than the thin walls (200 mm) (as shown in Fig. 6). Also, thicker walls failed at higher surface temperatures. The cooler region of the concrete infill delayed the failure time of the wall. The failure times for the models are compared in Table 2.

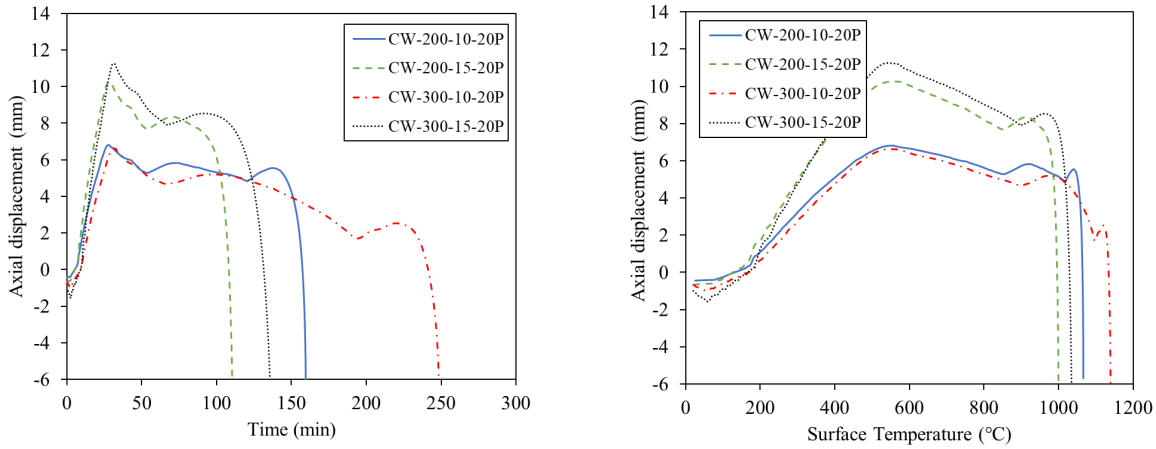


(a) Axial displacement against time (b) Axial displacement against surface temperature

Figure 7: The response of studied walls with various wall thickness and wall slenderness ratios.

## 5. Proposed Strength Design Equation

Observations from the parametric study were used to develop a method to calculate the axial compression strength of C-PSWs/CF at elevated temperatures. Two equations (Eq. 1 and 2) were proposed to estimate the axial compression capacity of C-PSWs/CF at elevated temperatures [$P_n(T)$]. The method considers temperature dependence of the concrete and steel modulus of elasticity and yield strengths. The comparison of both proposed equations with FE analysis results is described in this section.

$$P_n(T) = \left[ 0.32^{\left(\frac{P_{no}(T)}{P_e(T)}\right)^{0.3}} \right] P_{no}(T) \quad \text{(Lower bound)} \tag{1}$$

$$P_n(T) = \left[ 0.39^{\left(\frac{P_{no}(T)}{P_e(T)}\right)^{0.3}} \right] P_{no}(T) \quad \text{(Median)} \tag{2}$$

Where $P_{no}(T)$ is the cross-section nominal axial compressive strength at elevated temperatures and $P_e(T)$ is the elastic critical buckling load at elevated temperatures. $P_{no}(T)$ and $P_e(T)$ were computed using Eq. 3 and 4, respectively.

$$P_{no}(T) = A_s F_y(T) + \sum_{i=elements} 0.85 A_{ci} f_c'(T_i) \tag{3}$$

$$P_e(T) = \frac{\pi^2 EI_{eff}(T)}{(L_c)^2} \tag{4}$$

Where $A_s$ is the area of steel, $A_c$ is the area of concrete elements, $F_y(T)$is the yield strength of steel material at elevated temperatures and $f'_c(T)$ is the compressive strength of concrete at elevated temperatures. $L_c$ is the effective height of the wall. The effective stiffness of the composite section at elevated temperatures, $EI_{eff}(T)$, can be determined based on the temperature distribution through the thickness by using Eq.5.

$$EI_{eff}(T) = E_s(T)I_s + C_3 \sum_{i=elements} E_c(T_i)I_{ci} \quad (5)$$

$$C_3 = 0.45 + 3(A_s / A_g) \leq 0.9 \quad (6)$$

Where $A_g$ is the gross area of cross-section, $I_s$ is the moment of inertia of steel (faceplate), $I_c$ is the moment of inertia of concrete, $E_s(T)$ is the modulus elasticity of steel at elevated temperatures, $E_c(T)$ is the modulus elasticity of concrete at elevated temperatures and $C_3$ is the concrete contribution factor to the stiffness.

All the parameters were calculated based on the temperature of elements at the failure time for the studied cases in the parametric study. The determined axial compression strength of walls $P_n(T)$, was normalized to $P_{no}(T)$. The normalized axial strength loads were plotted against $P_{no}(T)/P_e(T)$ ratios. In Fig. 8, $P_n(T)/P_{no}(T)$ ratios against the $P_{no}(T)/P_e(T)$ ratios are plotted for all studied cases. Two equations were fitted to the data points obtained using FE analysis (parametric study). In Fig. 8, the proposed strength design equations are compared with FE analysis data points. Eq. 1 was defined as the lower bound which passes below all the data points. However, for Eq. 2 the average of the data points was considered in the curve fitting process. Therefore, the axial compressive strength of C-PSWs/CF at elevated temperatures can be predicted conservatively by using Eq. 1. The variation of the temperatures along the width of a wall is negligible. Hence, a 1-D heat transfer analysis can be conducted to calculate the temperatures through the wall thickness at the required fire resistance rating. Accordingly, $P_{no}(T)$ and $P_e(T)$ can be specified based on the determined through-thickness temperatures. Finally, the axial compressive capacity of a wall at the selected fire resistance rating can be computed.

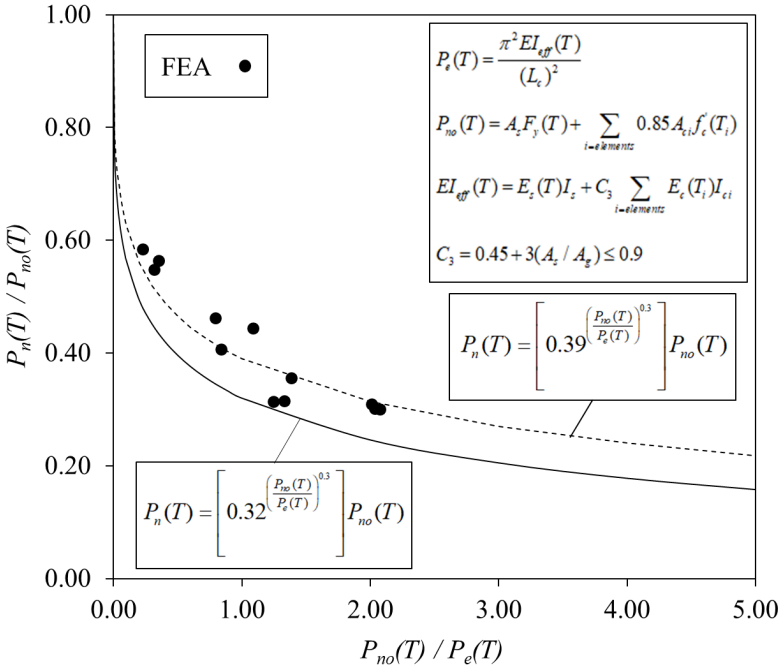

Figure 8: Proposed equations comparison with FE analysis results

## 6. Summary and Conclusions

C-PSWs/CF are being considered for high- rise commercial buildings. The stability of C-PSW/CF at elevated temperatures needs to be investigated. Detailed 3D finite element models for C-PSWs/CF were developed and benchmarked to existing experimental data for fire loading. Additional models were developed by considering unit-width column strips taken from the interior wall regions (regions with the lowest axial capacity). The column strip models were compared with whole specimen FE models and the experimental results. The column strip models conservatively estimate the capacity of the walls at elevated temperatures. The benchmarked strip models were then employed to conduct a parametric study to evaluate the effect of wall slenderness and wall thickness on the stability of C-PSWs/CF at elevated temperatures. The failure time of C-PSWs/CF increased with an increase in wall thickness due to cooler concrete regions in the middle of thicker walls. The failure time of C-PSWs/CF decreased with an increase in the wall slenderness ratio. The results from numerical studies were used to propose design strength equations based on unit width column strip calculations. A transient one-dimensional heat transfer analysis can be conducted to obtain temperature distribution through the thickness. The proposed equations can then be used to obtain the reduced axial compression strength per unit width of the wall at elevated temperatures.


## Acknowledgments

The project is funded by Charles Pankow Foundation, Steel Institute of New York (SINY) and American Institute of Steel Construction (AISC). The authors are grateful to these agencies for financial support. The authors also acknowledge the technical inputs received from the advisory panel.


## References


AISC (American Institute of Steel Construction). (2016). "Seismic Provisions for Structural Steel Buildings." AISC 341, Chicago, IL.

Alzeni, Y. and Bruneau, M. (2014). "Cyclic Inelastic Behavior of Concrete Filled Sandwich Panel Walls Subjected to In-Plane Flexure," *Technical Report MCEER-14-0009*, MCEER, University at Buffalo, Buffalo, NY.

ASCE *(*American Society of Civil Engineers). (2016). "*Minimum Design Loads for Buildings and Other Structure"ASCE 7.* Reston, VA.

Bhardwaj, S., Sharma, S., & Anvari, A. T., Varma, A. H (2019). "On the stability of composite plate shear walls under fire loading." *Proceedings of the Annual Stability Conference-Structural Stability Research Council,* St. Louis, MO, April 2-5, 2019

Bhardwaj, S.R., and Varma, A.H. (2016). "Effect of Imperfections on the Compression Behavior of SC Walls." *Proceedings of the Annual Stability Conference*, Structural Stability Research Council, Orlando, FL. April 12-15, 11 pp

Bhardwaj, S.R., and Varma, A.H. (2017a). "SC Wall Compression Behavior: Interaction of Design and Construction Parameters." *Proceedings of the Annual Stability Conference*, Structural Stability Research Council, San Antonio,Texas, March 2017, 14 pp.

Bhardwaj, S.R., and Varma, A.H. (2017b). "Design of Modular Steel-plate Composite Walls for Safety-related Nuclear Facilities." *AISC Design Guide 32*. American Institute of Steel Construction, Chicago, IL, USA

Bhardwaj, S.R., Varma, A.H., Orbovic, N. (2018a). "Behavior of Steel-plate Composite Wall Piers under Biaxial Loading." *Journal of Structural Engineering*, ASCE, Vol. 145, Issue 2, Feb. 2019. https://doi.org/10.1061/(ASCE)ST.1943-541X.0002247

Bhardwaj, S.R., Wang, A.Y., Varma, A.H. (2018b), "Slenderness Requirements for CF-CPSW: The Effects of Concrete Casting" in *Proceedings of Eighth International Conference on Thin-Walled Structures*, Lisbon,Portugal, 15 pp

Bruneau, M., Alzeni, Y., and Fouché, P. (2013). "Seismic behavior of concrete-filled steel sandwich walls and concrete-filled steel tube columns." *Steel Innovations 2013 Conf.*, Christchurch, New Zealand.

Cedeno, G., Varma, A.H., and Agarwal, A. (2009). "Behavior of Floor Systems under Realistic Fire Loading." *Proceedings of the 2009 Structures Congress, ASCE*.

Epackachi, S., Nguyen, N., Kurt, E., Whittaker, A. and Varma, A.H. (2015). "In-Plane Seismic Behavior of Rectangular Steel-Plate Composite Wall Piers." *Journal of Structural Engineering*, ASCE, Vol. 141, No. 7.

Eurocode (2005). "Eurocode 4: Design of Composite Steel and Concrete Structures–Part 1-2: General Rules Structural Fire Design." EN 1994-1-2, Brussels, Belgium.

Kurt, E.G., Varma, A.H., Booth, P.N. and Whittaker, A. (2016). "In-plane Behavior and Design of Rectangular SC Wall Piers Without Boundary Elements." *Journal of Structural Engineering*, ASCE, Vol. 142, No. 6.

Moon, I, Jee, N, Kim, W, Lee, C.S., Yoo, S.T. (2009). "Performance-based design of Stiffened Steel Plate Concrete Wall in Fire.". *Transactions of International Conference on Structural Mechanics in Reactor Technology*, *SMiRT 20*, Div. 6, Paper 1675, Espoo, Finland.

Ollgaard, J. G., Slutter, R. G., & Fisher, J. W. (1971). "Shear strength of stud connectors in lightweight and normal weight concrete." *AISC Eng'g Jr.,* April 1971 (71-10).

ISO-834 (*International Standard ISO 834*). (1975). "Fire resistance tests-elements-elements of building construction*."* Geneva, 1975.

Ji, X., Cheng, X., Jia, X., and Varma, A.H. (2017). "Cyclic In-Plane Shear Behavior of Double-Skin Composite Walls in High-Rise Buildings." *Journal of Structural Engineering*, Vol. 143, No. 6, ASCE, Reston,VA. https://doi.org/10.1061/(ASCE)ST.1943-541X.0001749

Selden, K. L. (2014). "Structural behavior and design of composite beams subjected to fire."

Selvarajah, R. (2013). "Behavior and design of earthquake-resistant dualplate composite shear wall systems." Ph.D. dissertation, Purdue Univ., West Lafayette, IN.

Seo, J., Varma, A. H., Sener, K., & Ayhan, D. (2016). "Steel-plate composite (SC) walls: In-plane shear behavior, database, and design." *Journal of Constructional Steel Research*, *119*, 202-215.

Simulia (2016). *ABAQUS 2017 Documentation*, Dassault Systemes Simulia Corporation Providence, RI.

Varma, A.H., Lai, Z., and Seo, J. (2017). "An Introduction to coupled composite core wall systems for high-rise construction." *Proceedings of the 8th International Conference on Composite Construction in Steel and Concrete*, Wyoming, USA.

Varma, A. H., Shafaei, S., & Klemencic, R. (2019). Steel modules of composite plate shear walls: Behavior, stability, and design. Thin-Walled Structures, 145, 106384.

Varma, A., Zhang, K., & Malushte, S. (2013). "Local Buckling of SC Composite Walls at Ambient and Elevated Temperatures." In *Transactions of the 22nd International Conference on Structural Mechanics in Reactor Technology (SMiRT 22)* (pp. 1-10).

Wang A., Seo J., Shafaei S., Varma A.H., and Klemencic, R. (2018). "On the Seismic Behavior of Concrete-Filled Composite Plate Shear Walls." *Eleventh U.S. National Conference on Earthquake Engineering*. Los Angeles, California, June 25-29, 2018.

Wei, F., Fang, C., & Wu, B. (2017). "Fire resistance of concrete-filled steel plate composite (CFSPC) walls." *Fire Safety Journal*, 88, 26-39.